Quantum Monte Carlo method for some model and realistic coupled anharmonic oscillators

M. Caffarel, P. Claverie,[a] and C. Mijoule
Dynamique des Interactions Moléculaires, Université Pierre et Marie Curie, Paris VI, Tour 22, 4 Place Jussieu, Paris Cedex 05, France

J. Andzelm[b] and D. R. Salahub
Département de Chimie, Université de Montréal, C. P. 6128, Succ. A, Montréal, Québec, H3C 3J7, Canada

(Received 27 October 1987; accepted 23 September 1988)

A new quantum Monte Carlo (QMC) method of evaluating low lying vibrational levels for coupled modes is presented. We use a modified fixed-node (FN) approach in which an extremum principle for energy levels is invoked. In this way, the nodal hypersurfaces of the nuclear wave function are parametrized and then optimized for each excited state. The method is tested on the fundamental excitations of some two-dimensional model potentials and is applied to the case of realistic coupled modes of the CO molecule adsorbed on a palladium cluster. The effect of an external electric field is also examined. The quantum Monte Carlo results are compared with those obtained in the conventional variational treatment of the nuclear Schrödinger equation for coupled vibrations. The QMC results give the exact values with an error which is in general less than 1 cm^{-1}. In all cases (even in the case of strong coupling) the use of our procedure leads to "optimal" nodal lines (in the sense of the extremum principle used in this work) which are practically undistorted. A salient feature of the Monte Carlo method presented here is that it readily permits the evaluation of the fundamental excitations of an arbitrary number of coupled vibrations. Furthermore, the potential energy surface may be represented by any analytical form without practical difficulties.

INTRODUCTION

In this paper a new method of evaluating vibrational energy levels is presented. Our goal is to overcome the limitations of the usual variational approaches. Two important limitations must be pointed out. The first is related to the difficulty of taking into account strong anharmonicity of the potential energy surface. Strong anharmonicity generally yields too slow convergence of the variational calculation.[1] A second limitation occurs when a large number of interacting vibrations has to be treated. Indeed, the rapid increase of memory and CPU time requirements limits realistic calculations to a small number of vibrations (typically not more than three). Problems related to the quality of the fitting procedure of the potential may also be troublesome in variational approaches.

The new approach is developed within the very general framework of a pure diffusion quantum Monte Carlo (QMC) method using a full generalized Feynman–Kac (FGFK) formula.[2–5] This method is referred to in the following as the FGFK-QMC method. That method, originally designed for treating the electronic structure of atoms and molecules, is here adapted to the multimode vibrational problem. A widely used approach for treating molecular vibrations is the well-known "normal mode approximation" using an approximate Hamiltonian.[6] However, if accurate results are desired this description must be abandoned and the entire potential energy hypersurface must be considered. In this situation a new difficulty arises, namely the loss of any kind of symmetry for the Hamiltonian. We are then led to the problem of evaluating some "genuine" excited levels, i.e., excited states which cannot be considered as the ground state in a given symmetry subspace. This problem is not a trivial one for Monte Carlo schemes. In order to take it into account, we present here a generalization of the well-known fixed-node approximation.[4,5,7] This approach is currently used to determine properties of the ground state in a symmetry subspace (the so-called "fermionic" ground states corresponding to a given total spin for atoms and molecules[4]). In this paper the method is first tested on some model potentials including intermediate or strong anharmonic coupling terms. Then the first applications are presented which are drawn from a realistic potential surface involving the vibrations of a chemisorbed molecule. Both cases illustrate the efficiency and the simplicity of the method. In particular, in light of the results, it now seems reasonable to hope for solutions of the vibrational problem for an "arbitrary" surface and an arbitrary number of coupled (even strongly coupled) vibrations accurate to about 1 cm^{-1} for the ground state energy (or zero point energy) and for some of the lower-lying excited levels.

The organization of the paper is as follows. We first summarize the main features of the basic quantum Monte Carlo method used here. The detailed theory including mathematical derivations may be found elsewhere.[2–5] Second, we present the fixed-node approximation in the framework of the FGFK-QMC method and our generalization to

[a] Deceased, January 24, 1988.
[b] Present address: Cray Research Inc., 1333 Northland Drive, Mendota Heights, Minnesota 55120.

 0021-9606/89/020990-13$02.10

the case of the determination of genuine excited levels. Third, the method is tested on some numerically solvable problems. Finally, we present some realistic numerical applications. The preliminary results presented here should be understood primarily as a comparison between the two methods, the classical variational and our new QMC approach. Their physical implications and comparisons with various experiments will, in due course, be treated separately.

II. OUTLINE OF THE QUANTUM MONTE CARLO METHOD

The method is based on the use of a pure diffusion process and a generalized Feynman–Kac formula. The underlying diffusion process is built from a so-called "reference function" $\varphi_0^{(0)}$ which is chosen as close as possible to the exact wave function to reduce the statistical error (see, e.g., Refs. 5 and 7).

The reference diffusion process is completely determined by its drift vector $\mathbf{b}$ and diffusion constant $\mathscr{D}$. These quantities are written in terms of the reference function as follows (atomic units $\hbar = 1$, $e = 1$, $m_e = 1$ are used throughout the paper):

$$\mathbf{b} = \nabla\varphi_0^{(0)}/\varphi_0^{(0)}, \tag{1a}$$

$$\mathscr{D} = 1. \tag{1b}$$

From the Langevin equation associated with the reference diffusion process, stochastic trajectories may be generated using a step-wise procedure (see, e.g., Ref. 9 Sec. 3.6)

$$d\mathbf{X}(t) = \mathbf{b}[\mathbf{X}(t)]dt + \mathscr{D}^{1/2}d\mathbf{W} \tag{2a}$$

with the discretized version corresponding to the time step Δt:

$$\Delta\mathbf{X}(t) = \mathbf{b}[\mathbf{X}(t)]\Delta t + \mathscr{D}^{1/2}\Delta\mathbf{W}(\Delta t), \tag{2b}$$

where $\mathbf{W}$ represents the multidimensional Wiener process and $\mathbf{b}$ and $\mathscr{D}$ the drift vector and diffusion constant defined in Eqs. (1) [$\Delta\mathbf{W}(\Delta t)$ is a multidimensional Gaussian random vector whose components verify $\langle\Delta W_i\rangle = 0$ and $\langle\Delta W_i \Delta W_j\rangle = \delta_{ij}\Delta t$)].

In this work we use a simplified form of the full generalized Feynman–Kac formula presented elsewhere,[4] namely

$$I(t) = \langle\varphi_0^{(0)}|e^{-t(H-E_0^{(0)})}|\varphi_0^{(0)}\rangle = \int_{\Omega(t)} \exp\left[-\int_{-t/2}^{t/2} V_p[X(s)]ds\right] D^{\varphi_0^{(0)}}X. \tag{3}$$

This formula expresses a quantum matrix element of the evolution operator (in imaginary time) $\exp(-tH)$ as a functional integral involving the diffusion measure of the reference diffusion process. $\Omega(t)$ denotes the set of continuous trajectories defined in the time interval $(-t/2, +t/2)$, while the diffusion measure is noted $D^{\varphi_0^{(0)}}X$. The function V_p is the so-called perturbing potential given by

$$V_p = V - E_0^{(0)} - (1/2)\nabla^2\varphi_0^{(0)}/\varphi_0^{(0)}, \tag{4}$$

where V is the potential energy of the system to be studied and $E_0^{(0)}$ an arbitrary constant [in actual fact, V_p is nothing but $V - V^{(0)}$, where $V^{(0)}$ denotes the "reference potential energy" of the reference Hamiltonian $-\nabla^2/2 + V^{(0)}$, associated with the reference function $\varphi_0^{(0)}$ as described in Refs. 4 and 5].

If the reference function is chosen square integrable (and this will always be the case in the following), then the associated diffusion process is ergodic[4] and the functional integral appearing in Eq. (3) may be evaluated as a time average along any stochastic trajectory $X^{(0)}(s)$ of the process. We thus write

$$I(t) = \int_{\Omega(t)} \exp\left[-\int_{-t/2}^{t/2} V_p[X(s)]ds\right] D^{\varphi_0^{(0)}}X = \lim_{T\to+\infty}(1/T) \times \int_0^T \exp\left[-\int_{-t/2+\tau}^{t/2+\tau} V_p[X^{(0)}(s)]ds\right] d\tau. \tag{5}$$

Note that, according to the ergodic property of the diffusion process, it is possible, instead of a single, very long stochastic trajectory, to use a set of shorter trajectories. In practice, this possibility enables us to obtain an evaluation of the variance using standard statistical methods.

In fact, as concerns the ergodic property, two different cases must be properly distinguished. If the reference function does not vanish at any finite distance, the property readily holds and any arbitrary stochastic trajectory may be used. If not, it is necessary to take account of consequences resulting from divergence of the drift vector [Eq. (1a)] at nodes of $\varphi_0^{(0)}$. Indeed, nodal hypersurfaces of $\varphi_0^{(0)}$ play the role of infinitely repulsive barriers for stochastic trajectories. There then results a decomposition of the diffusion process into a juxtaposition of subprocesses in subdomains delimited by the nodes of the reference function. In other words, an arbitrary stochastic trajectory cannot leave a subdomain in which it is trapped and accordingly, cannot visit everywhere. Property (5) must then be applied, not by using a single trajectory, but a set of trajectories consisting of at least one trajectory trapped in each subdomain. The whole space is accordingly sampled.

Now, the quantum matrix element $I(t)$ may be written in terms of the spectral expansion of H thus leading to

$$I(t) = \langle\varphi_0^{(0)}|e^{-t(H-E_0^{(0)})}|\varphi_0^{(0)}\rangle = \sum |\langle\varphi_0^{(0)}|\varphi_i\rangle|^2 e^{-t(E_i-E_0^{(0)})}. \tag{6}$$

E_i and φ_i denote, respectively, the eigenvalues and eigenfunctions of H.

The summation sign Σ is here a shorthand notation which may represent either a discrete summation or a continuous integration. The spectrum of H can be obtained by analyzing $I(t)$ into a sum of real exponentials. Let us denote as E_{i_0} the lowest energy associated with a nonvanishing overlap integral $\langle\varphi_0^{(0)}|\varphi_i\rangle$. Extracting E_{i_0} may be done as follows:

$$E_{i_0} = E_0^{(0)} - \lim_{t\to+\infty}(1/t)\log I(t). \tag{7}$$

A much more efficient way consists in considering the slope at infinity of $\log I(t)$:

$$E_{i_0} = E_0^{(0)} - [\log I(t_2) - \log I(t_1)]/(t_2 - t_1) + O(e^{-\Delta E t_1}) \quad (8)$$

with $t_2 > t_1$. ΔE denotes the energy difference between E_{i_0} and the first excited energy associated with a nonvanishing overlap $\langle \varphi_0^{(0)} | \varphi_i \rangle$. The residual error may be made arbitrarily small by using a large enough value of t_1.

Finally, the complete algorithm is as follows:

—choose some good representation of the exact wave function as reference function $\varphi_0^{(0)}$;

—generate stochastic trajectories using the Langevin equation (2);

—evaluate $I(t)$ expressed as a time average along the previous trajectories using the basic formula (5);

—extract the desired energy according to formula (8).

At this stage, it is of interest to note that the present quantum Monte Carlo method differs from other similar methods (e.g., Refs. 7 and 8) essentially because no branching is introduced. Indeed, the reference diffusion process used here coincides with their branching-diffusion process when the branching term is removed [see, e.g., Eq. (6) in Ref. 7] and if our reference function $\varphi_0^{(0)}$ is identified to their "trial wave function" Ψ_T. In addition, our perturbing potential V_p [Eq. (4)] may be rewritten in the equivalent form

$$V_p = H\Psi_T/\Psi_T$$

which corresponds exactly to the "local energy" used in these methods.

III. EVALUATION OF VIBRATIONAL ENERGY LEVELS

A. Zero-point energy (ZPE)

Ground state energies are very simply and accurately evaluated by all Monte Carlo schemes. This salient feature is directly related to the lack of nodes in the ground state wave function (see, e.g., Ref. 10). As a consequence, the algorithm presented in the previous section may be readily used. A few excellent results for zero-point energies are presented below.

B. Fixed-node approximation and excited levels

In this section we are interested in evaluating energies of excited levels. We will denote as φ_{i_0} the corresponding excited-state wave functions. By contrast with the previous case, we are now dealing with wave functions with nodes. It can be shown that the algorithm defined above may be used in the same way as for the ground state energy.[4] The basic difference concerns the drift vector of the reference diffusion process which may now diverge. Accordingly, eigensolutions determined by the Monte Carlo scheme correspond to eigensolutions of the Schrödinger equation constrained to vanish everywhere the reference function vanishes. This must be understood as a change in boundary conditions for the Schrödinger equation. Consequently, the energies obtained in this way may differ from the exact ones. This is the well-known fixed-node approximation.[4,5,7]

Let ν_α denote the hypervolumes delimited by the nodes of the reference function $\varphi_0^{(0)}$ and S_α the corresponding boundary hypersurfaces. From the continuity of $\varphi_0^{(0)}$ it follows that

$$\mathbf{R}^N = \bigcup_{\alpha=1}^{l} \nu_\alpha, \quad (9)$$

where N is the dimension of the relevant space. In what follows, N will represent the number of coupled modes. l is the number of hypervolumes.

As explained above, the Schrödinger equation is solved (through the Monte Carlo procedure) *independently* in each volume ν_α. Let us denote as Φ_α the different nodeless solutions in subdomains ν_α and as ϵ_α the corresponding energy:

$$H\Phi_\alpha = \epsilon_\alpha \Phi_\alpha \quad \mathbf{r} \in \nu_\alpha, \quad (10a)$$

$$\Phi_\alpha = 0 \quad \mathbf{r} \notin \nu_\alpha. \quad (10b)$$

Note that Φ_α may have a discontinuous gradient at the nodal hypersurface S_α.

The functional integral involved in the Feynman–Kac formula may be decomposed into a sum of functional integrals defined over the set of continuous trajectories $\Omega_\alpha(t)$ trapped in a given subdomain ν_α. We thus write

$$I(t) = \sum_\alpha w_\alpha I_\alpha(t), \quad (11)$$

where the w_α's denote the relative statistical weights of the different subdomains ν_α which are immediately obtained from the stationary density $(\varphi_0^{(0)})^2$ associated with the reference function $\varphi_0^{(0)}$:

$$w_\alpha = \int_{\nu_\alpha} (\varphi_0^{(0)})^2 \, d^N x \Big/ \int_{\mathbf{R}^N} (\varphi_0^{(0)})^2 \, d^N x \quad (12)$$

and $I_\alpha(t)$ denotes the "partial" functional integral

$$I_\alpha(t) = \int_{\Omega_\alpha(t)} \exp\left[-\int_{-t/2}^{t/2} V_p[X(s)] ds \right] D^{\varphi_0^{(0)}} X. \quad (13)$$

Using the Feynman–Kac formula $I_\alpha(t)$ may also be expressed as a quantum matrix element. The spectral expansion (6) for $I_\alpha(t)$ combined with the expression (11) for $I(t)$ leads to the following expression for the fixed-node energy E_{FN}:

$$E_{\mathrm{FN}} = E_0^{(0)} - \lim_{t \to +\infty} (1/t) \log I(t) = \min_\alpha \epsilon_\alpha. \quad (14)$$

If exact nodes were known, the fixed-node approximation would be exact and we should thus obtain

$$E_{\mathrm{FN}} = \epsilon_1 = \cdots = \epsilon_\alpha = \cdots \epsilon_l = E_{i_0}. \quad (15)$$

In the general case of approximate nodes, E_{FN} is different from the exact result E_{i_0}.

In previous work, the fixed-node approach has been introduced in order to evaluate energies corresponding to ground states in subspaces of given symmetry. It is then possible to show that a variational property holds,[7,11] namely

$$E_{\mathrm{FN}} = \min(\epsilon_\alpha) \geqslant E_{i_0}. \quad (16)$$

As already mentioned, the excited levels of multivibrational systems are generally *true* excited energies. No symmetry holds and the upper-bound property is no longer valid.

We have therefore developed a generalization of the fixed-node approach for such true excited levels. This generalization rests on the extremum property associated with *all* eigenvalues of the Schrödinger Hamiltonian. This property states that[12,13]

$$E(\varphi_k + \delta\varphi) = E(\varphi_k) + O(\delta\varphi^2), \tag{17}$$

where $E(\varphi)$ is the usual energy mean value

$$E(\varphi) = \langle\varphi|H|\varphi\rangle/\langle\varphi|\varphi\rangle \tag{18}$$

and φ_k is an arbitrary eigenstate of H. Note that the widely used property of *minimum* energy is valid only for the ground state energy E_0. Now, in order to use this extremum property we must establish an *a priori* nontrivial connection between the quantum mean value $E(\varphi)$ and the fixed-node energy $E_{\rm FN}$ evaluated in the Monte Carlo scheme. As emphasized above, the resolution of the Schrödinger equation is done *independently* in each volume. As a consequence the relative magnitude of the different solutions Φ_α in different subdomains is *not* determined by the fixed-node procedure. More precisely, the set of coefficients $\{c_\alpha\}$ such that the function φ defined as

$$\varphi = \sum_\alpha c_\alpha \Phi_\alpha \tag{19}$$

is close to the desired exact wave function φ_{i_0} is unknown. From Eqs. (18) and (19) we obtain the following energy mean value for φ:

$$E(\varphi) = \sum_\alpha c_\alpha^2 \epsilon_\alpha \langle\Phi_\alpha|\Phi_\alpha\rangle \Big/ \sum_\alpha c_\alpha^2 \langle\Phi_\alpha|\Phi_\alpha\rangle. \tag{20}$$

Note that delta functions due to the possibly discontinuous gradient of Φ_α do not contribute to the numerator (because these discontinuities of the gradient can occur only on the boundaries, where the Φ_α's just vanish themselves). The important point now is that the coefficients c_α do not have to be known if the Monte Carlo energies ϵ_α have a common value. More precisely, we obtain from Eq. (20) in this particular case:

$$E(\varphi) = E_{\rm FN} = \epsilon_1 = \epsilon_2 = \cdots = \epsilon_l. \tag{21}$$

Consequently, if Eq. (21) is verified it is possible to apply the extremum principle to the fixed-node energy. The method presented in this paper is essentially based on this latter remark and thus consists in extremizing the fixed-node energy with respect to some deformations of nodes with the constraint that the energies have a common value. In what follows, the reference function will be written in the general form

$$\varphi_0^{(0)} = f(x_1,...,x_N;p_1,...,p_q)e^{-\phi(x_1,...,x_N)}, \tag{22}$$

where ϕ is a bounded function at any finite distance and $f=0$ defines the $(N-1)$-dimensional nodal hypersurface which is parametrized by $p_1,..., p_q$. In order to apply the constrained extremum principle, the set of parameters $\{p_i\}_{i=1,q}$ is decomposed into two subsets $\{p_i\}_{i=1,r}$ and $\{p_i\}_{i=r+1,q}$. The variation of the fixed-node energy is performed with respect to the subset $\{p_i\}_{i=r+1,q}$ while for each given $\{p_i\}_{i=r+1,q}$ the parameters $\{p_i\}_{i=1,r}$ are only used to fulfill the constraint (21). The theoretical algorithm of the method is then as follows: (1) For a given subset of fixed parameters $\{p_i\}_{i=r+1,q}$, vary parameters $\{p_i\}_{i=1,r}$ to obtain equality of energies $\{\epsilon_\alpha\}_{1,l}$. Each of energies ϵ_α may be evaluated by Monte Carlo according to Eq. (14) from a set of trajectories trapped in the corresponding subdomain ν_α so that $I(t) = I_\alpha(t)$ and $E_{\rm FN} = \epsilon_\alpha$. The common value for the energies will be denoted as $\epsilon(p_{r+1},...,p_q)$. According to Eq. (21), this step assures that $\epsilon(p_{r+1},...,p_q) = E(\varphi)$ where φ is a function close to the exact wave function φ_{i_0}. (2) Repeat step 1 for different subsets $\{p_i\}_{i=r+1,q}$. (3) According to the extremum principle [Eq. (17)], deduce E_{i_0} as a local extremum of $\epsilon(p_{r+1},...,p_q)$.

Although such a theoretical algorithm is simple and general, its practical implementation may lead to serious difficulties. In fact, the most important problem consists in constructing a reference function whose nodes are close enough to the exact ones to justify the use of the extremum property [Eq. (17)]. Such a construction is by no means a trivial task since the nodal hypersurface of the exact wave function cannot be known *a priori* and may be obtained only by solving the Schrödinger equation. In general, the topological structure of the nodal hypersurfaces is complicated and may be difficult to reproduce, particularly when arbitrarily high energy levels are considered. Even the number of subdomains delimited by nodes is generally unknown. If exact nodes were known, the constraint (21) would be automatically fulfilled. It is natural to think that for very good nodes this is still possible. In contrast, if parametrized nodes are not close to the exact nodes, as is the case in general, it may be very difficult to fulfill this constraint even by using a large number of parameters. In addition, if Eq. (21) is satisfied, there can be several extrema for the energy and the problem of choosing between them arises. Such unwanted additional extrema may correspond to other physical levels or, perhaps, to artificial extrema in functional space. All the problems listed above illustrate the difficulty in applying the previous theoretical algorithm to an arbitrary multimode problem. However, in this paper we will restrict ourselves to the problem of evaluating the so-called fundamental energies of the system. A convenient way of defining fundamental energies is to introduce the Hamiltonian consisting of the noncoupled part of the total Hamiltonian, namely

$$H^{\rm NC} = \sum_{i=1}^N h_i(x_i) = \sum_{i=1}^N -\frac{1}{2}\frac{\partial^2}{\partial x_i^2} + V_i(x_i) \tag{23}$$

while the total Hamiltonian will be written in the form

$$H = H^{\rm NC} + \lambda W(x_1,...,x_N). \tag{24}$$

Eigenfunctions and eigenvalues of $H^{\rm NC}$ are given by

$$\phi_{k_1\cdots k_N}(x) = \prod_{j=1}^N \varphi_{k_j}^{(j)}(x_j) \tag{25}$$

and

$$E_{k_1\cdots k_N} = \sum_{j=1}^N \epsilon_{k_j}^{(j)}, \tag{26}$$

where $\varphi_{k_j}^{(j)}$ and $\epsilon_{k_j}^{(j)}$ denote the eigensolutions of the one-dimensional oscillators defined by h_j. The fundamental ener-

gies of the noncoupled Hamiltonian are defined as the energies corresponding to $k_j = 1$, all other k's being zero. The energy levels of H which are connected to the previous ones as the perturbation parameter λ goes to zero are called fundamental energies of H. In what follows, these energies will be denoted as $E_{(0,\ldots,1,\ldots,0)}$. Denoting by $E_{(0,\ldots,0,\ldots,0)}$ the ground state energy (or zero-point energy), the differences: $E_{(0,\ldots,1,\ldots,0)} - E_{(0,\ldots,0,\ldots,0)}$ will be referred to as the fundamental excitations of the system. Now, it is important to point out that these excitations play a central role in spectroscopy because they are generally the more intense. Due to the inherent limitations of the variational approach, it would be valuable to be able to compute them accurately for problems in which many modes are involved. For that, we apply the previous theoretical algorithm by using a basic assumption concerning the nodal structure of wave functions corresponding to fundamental excitations. More precisely, it will be assumed here that nodes of such functions may be correctly approximated by a hypersurface dividing the N-dimensional space into exactly *two* subdomains. It is known that such a representation of nodes is exact for the first excited state of H[19] (which corresponds here to one of the fundamental energies) but is generally wrong for other levels. As concern the true fundamental energies, we have seen that they are connected to the fundamental energies of the noncoupled Hamiltonian by their very definition. But it is clear that fundamental energies of H^{NC} correspond to wave functions which verify the basic assumption. It is then assumed here that adding a coupling potential [such as $W(x)$ given in Eq. (24)] does not destroy in an abrupt way the nodal pattern of fundamental wave functions. In what follows, this assumption is tested by treating some two-dimensional model problems in which the magnitude of $W(x)$ (the coupling potential) may be very important and for fundamental energies which do not necessarily correspond to a first excited state. Let us denote the "excited" mode as x_1. Invoking our basic assumption the nodal function f is represented as follows:

$$f(x_1,\ldots,x_N,p_1,\ldots,p_q) = x_1 + p_1 + g(x_2,\ldots,x_N,p_2,\ldots,p_q). \quad (27)$$

Clearly, the function f divides the N-dimensional space into two subdomains. Let us denote ϵ_1 and ϵ_2 the two corresponding energies. In what follows, p_1 will correspond to the single parameter used to fulfill the constraint of Eq. (21), that is here $\epsilon_1 = \epsilon_2$. Parameters $p_2,\ldots, p_q$ are introduced to extremize the common value $\epsilon(p_2,\ldots, p_q)$. As concerns the function g, it may be developed as increasing powers of the x_i and then successive improvements of g may be made. For instance

$$g^{(0)} = 0, \quad (28a)$$

$$g^{(1)} = \sum_i p_i x_i, \quad (28b)$$

$$g^{(2)} = g^{(1)} + \sum_{i,j} p_{ij} x_i x_j, \quad (28c)$$

and so on. Increasing the order of g should yield a "better" representation of the nodes and, finally, a converged optimized energy. In contrast to the theoretical algorithm presented above for a very general energy level, it is important to note that no basic difficulties arise from such an algorithm in which only two subdomains are introduced. Its practical implementation may thus be considered.

IV. APPLICATION TO TWO-DIMENSIONAL SYSTEMS

In order to test the theoretical algorithm described above, the fundamental excited states of some two-dimensional model potentials have been investigated. They were chosen in such a way that the exact solutions may be reached by the variational method. Both intermediate and strong coupling potentials are studied.

Furthermore, the method has been applied to some surface science problems involving vibrations of the CO molecule adsorbed on palladium. In the first instance adsorption on the bridge site of a 14-atom cluster model of Pd (100) was considered.[14,15] A second example involves the bridge-bonded Pd_2CO cluster in the presence of an external electric field.[16] In each case the coupling of two modes has been considered.

Throughout the paper the $|N_1,N_2\rangle$ normal mode notation is used, where N_1, N_2 refer to the harmonic oscillator quantum numbers of the first and second vibrations, respectively. In this paper we are interested in the fundamental excitations for the system. We are then led to evaluate $E_{(0,0)}$, $E_{(0,1)}$, and $E_{(1,0)}$ for each couple. In each case both variational and QMC methods are applied.

A. Model potentials

First we have to compare the QMC calculations with energies which may be reached exactly by numerical calculations. Polynomial forms of potentials have therefore been chosen, where the ground and excited energies may be readily obtained by a variational calculation. In order to study both symmetrical and unsymmetrical excited states, the first kind of potentials we chose have the following analytical form:

$$V_{\mathrm{I,II}}(x,y) = x^2 + y^2 + \lambda(-xy^2 + y^4). \quad (29)$$

The shape of the nodal line of the $|1,0\rangle$ excited state is unknown, whereas that of the symmetrical $|0,1\rangle$ level is given by $y = 0$. The coupling between x and y is governed by the parameter λ. Two values of λ have been considered, $\lambda = 1$ (V_{I}) and $\lambda = 3.5$ (V_{II}). In any case, λ is chosen so that the potential has only one minimum and no unbound states to assure the convergency of the variational treatment. It is straightforward to show that these two properties are fulfilled for $0 \leqslant \lambda < 4.0$. Furthermore, in order to study the effect of long-range coupling on the shape of the nodal line of the unsymmetrical excited state $|1,0\rangle$, the following form of V has also been studied:

$$V_{\mathrm{III}}(x,y) = x^2 + y^2 + \lambda(-xy^2 + x^2y^2 + y^4). \quad (30)$$

Indeed, although the two oscillators associated with V_{I} and V_{II} are decoupled for large values of x and y, they remain strongly coupled in the case of V_{III}.

As discussed below, the potentials V_I, V_{II}, and V_{III} have their unsymmetrical $|1,0\rangle$ state as the lowest excited level. In order to investigate the accuracy of Eq. (27) for higher excited unsymmetrical states, the last model example we treated is the following potential:

$$V_{IV}(x,y) = 4x^2 + 0.1y^2 + \lambda(-xy^2 + y^4) \qquad (31)$$

with $\lambda = 3.5$. In this more general case, the intrinsic properties associated with a first excited state (i.e., the partitioning of the space into two subdomains) are eventually removed.

B. Realistic potentials

For the $Pd_{14}CO$ study, the first mode involves the beating of the rigid CO molecule against the surface (denoted h on Fig. 1). The second coordinate is a surface mode of the metal cluster, either the out-of-plane Pd_2–bulk stretch (z on Fig. 1) or the in-plane Pd–Pd stretch (r on Fig. 1). In the electric field study we have focused on the CO stretch (coordinate d on Fig. 2) and its coupling with the surface–CO beating vibration (h). We calculated total energy surfaces as a function of h,r, h,z, and h,d, respectively. In each case the potential surface was evaluated on a two-dimensional grid of about 40 points using the LCGTO-MP-LSD method developed elsewhere.[14,17] The points were chosen to bracket the ground and first excited vibrational levels. Furthermore, for large values of h, the asymptotic form of the potential was taken into account by adding to the grid,four or five points at distances beyond 10 Å, derived from the known experimental chemisorption energy of CO on the Pd (100) surface. The supplementary points are introduced to prevent an unphysical asymptotic behavior of the polynomial fit to the potential, namely a fourth-order polynomial using a least-squares fit method[18]:

$$V(x_1,x_2) = \sum_{i+j<4} a_{ij} x_1^i x_2^j. \qquad (32)$$

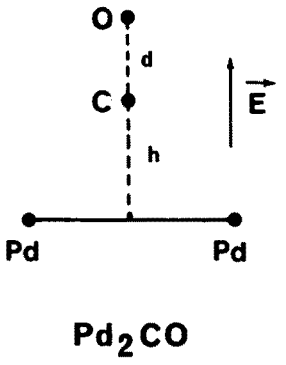

FIG. 2. Representation of the couple h,d. The study of this coupling is performed in presence of an external electric field E.

C. Variational treatment

The variational equations are solved explicitly using a Hermite polynomial expansion as described elsewhere.[18] The effect of the basis size is studied. The polynomial representation of the potential allows easy calculations of the matrix elements of the nuclear Hamiltonian. However, concerning realistic potentials, such a mathematical expansion, suitable for small displacements, may lead to nonphysical behavior of the potential at large distances. This is the case for the h,z system where the coupling is significant. As a consequence, large basis set calculations using very delocalized Hermite polynomials are prohibited. Consequently, we are led to contract the basis set significantly in order to assure that the process converges in the region of space where the potential is physically well described. Since the QMC method does not involve the evaluation of matrix elements over a basis, the computational constraints on the form of the potential are much less severe. More precisely, according to formulas (4) and (5) only the successive values of the potential V along the trajectory are needed and then an arbitrary analytical form of V may be chosen. It is then possible to introduce more physical expressions for V with the right

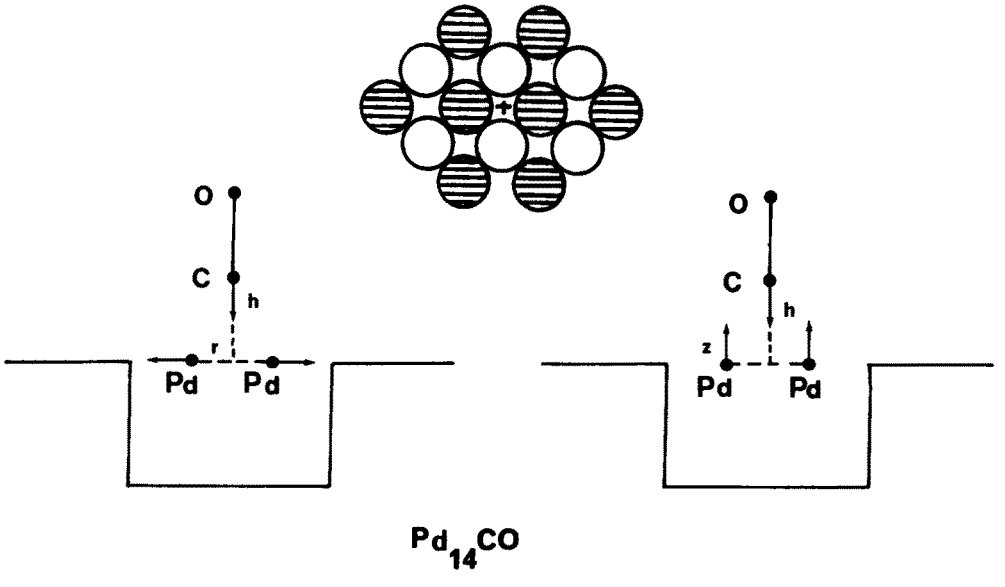

FIG. 1. Representation of the $Pd_{14}CO$ cluster and couples h,r and h,z. The dashed Pd atoms belong to the first layer. The CO chemisorption site is indicated by the cross.

asymptotic behavior (i.e., Morse functions for stretching modes, Fourier expansions for multiple-wells potentials, etc.). However, as the purpose of this paper is to compare both variational and QMC methods, the form (32) above is used in all cases. Concerning the h,z potential, the reference functions are chosen so that the nonphysical part of the potential cannot be visited by the stochastic trajectories during the Monte Carlo simulation. This is accomplished by using reference functions nearly vanishing in these pathological regions of the potential fit. In this way, a "local convergency" may be reached. By local convergency it is meant here that we obtain the energy corresponding to a new problem represented by the physical potential surface around the potential well and infinite repulsive barriers at large distances. If very long Monte Carlo runs would be performed, these pathological regions would, in fact, be visited and the energy would converge to a nonphysical value (which can be equal to $-\infty$ if the nonphysical part of the potential is not bounded from below). It is very important to emphasize that these difficulties occur only because an inadequate polynomial fit is used. Such difficulties do not occur for more physical potentials. As remarked above, reasonable physical potentials may be readily used, without practical difficulties, in the Monte Carlo approach since no complicated matrix elements have to be evaluated. This is one of the main advantages of QMC methods. In the following a unitary transformation $(x_1,x_2) \rightarrow (x_1',x_2')$ is performed on the three realistic potentials such that the a_{11} coefficient in Eq. (32) vanishes. These new coordinates will be called "pseudonormal coordinates" (PNC).

D. QMC treatment

Concerning the nodeless vibrational ground states $|0,0\rangle$ the choice of the reference function $\varphi_0^{(0)}$ is rather flexible, the statistical fluctuations becoming rapidly small. $\varphi_0^{(0)}$ is written in the following form:

$$\varphi_0^{(0)}(x_1,x_2) = e^{-k_1x_1^2 - k_2x_2^2}, \tag{33}$$

where (x_1,x_2) stands for h',r', h',z', or h',d'. The reference function for excited states $|0,1\rangle$ and $|1,0\rangle$ is chosen as follows:

$$\varphi_0^{(0)}(x_1x_2) = f(x_1,x_2)e^{-k_1f^2(x_1,x_2) - k_2x^2}, \tag{34}$$

where x_1 refers to the excited vibration. When choosing the function f the boundary conditions of $\varphi_0^{(0)}$ at infinity must be satisfied. $f(x_1,x_2) = 0$ is the equation defining the nodal structure of the reference function. As explained in Sec. III B, in the following the nodes of the states $|0,1\rangle$ and $|1,0\rangle$ are represented by a line dividing the two-dimensional space into two domains. As a general rule, this representation, which is exact for the first excited state of the Hamiltonian, is wrong for the higher excited states.[19] Nevertheless, the approximation associated with this representation is expected to be good when excited states under consideration correspond to the first excitation of a given vibration (denoted as $|0,1\rangle$ and $|1,0\rangle$). Note that the function f appears in the exponential part and allows the maximum of $\varphi_0^{(0)}$ to keep a constant distance from the nodal line when it is moved. At the beginning of our investigation, in order to describe as well as possible the nodal surface with the generalized fixed-node approximation, only small deformations and displacements of the nodal line about the straight line $x_1 = 0$ have been performed. The approximate form for $f(x_1,x_2)$ is chosen by expanding the development given in Eqs. (28) to the second order. We may then write f as

$$f(x_1,x_2) = x_1 - \alpha x_2^2 - x_N, \tag{35}$$

where x_N is related to the translation of the nodal line while αx_2^2 corresponds to a small parabolic deformation. Linear terms (rotation of the nodal line) corresponding to $g^{(1)}$ [Eq. (28b)] are zero for the model potentials and are negligible in the PNC representation of the realistic h,r and h,z potentials.

In order to apply the generalized fixed-node (GFN) algorithm described in Sec. III B to our examples the following steps are performed: (i) for each value of α the equality $\epsilon_1 = \epsilon_2 = \epsilon(\alpha)$ is obtained by varying x_N, (ii) the extremum principle is used for optimizing $\epsilon(\alpha)$ with respect to α.

In order to reduce as much as possible the variance of the QMC procedure, at each step described above the k_1 and k_2 parameters in Eq. (34) are adjusted to minimize the variance by performing short-time preliminary runs using a common underlying sequence of random numbers.

V. RESULTS OF THE VARIATIONAL AND QMC CALCULATIONS

A. Model potentials

The analytical form of the model potentials studied are summarized in Table I. The potential map of V_{II} is represented in Fig. 3 as an example. In Table II, different approaches of the ground and fundamental excited states of V_{II} are compared with QMC, namely, the crude harmonic approximation and the variational procedure. The effect of the basis set size for the latter is also reported. All the calculated energies as well as the optimized nodal lines at the second-order level are reported in Table III for all studied potentials. Concerning the ground state energies, it is clear that they are very well reached by variational calculations and that QMC runs converge rapidly as a function of the simulation time T as shown in Fig. 4. An accuracy better than 1 cm^{-1} is very easy to obtain. Such results will allow the method to be extended without difficulties to physical problems where a good evaluation of the zero-point energy (ZPE) for a high dimensional system is necessary.

TABLE I. Polynomial model potentials for which the ground state and fundamental excitations have been investigated.[a]

Coefficients[b]	V_I	V_{II}	V_{III}	V_{IV}
a_{20}	1.0	1.0	1.0	4.0
a_{02}	1.0	1.0	1.0	0.1
a_{12}	−1.0	−3.5	−3.5	−3.5
a_{22}	0.0	0.0	3.5	0.0
a_{04}	1.0	3.5	3.5	3.5

[a]Mass normalized coordinates are used.
[b]Atomic units. All the missing coefficients are set to zero.

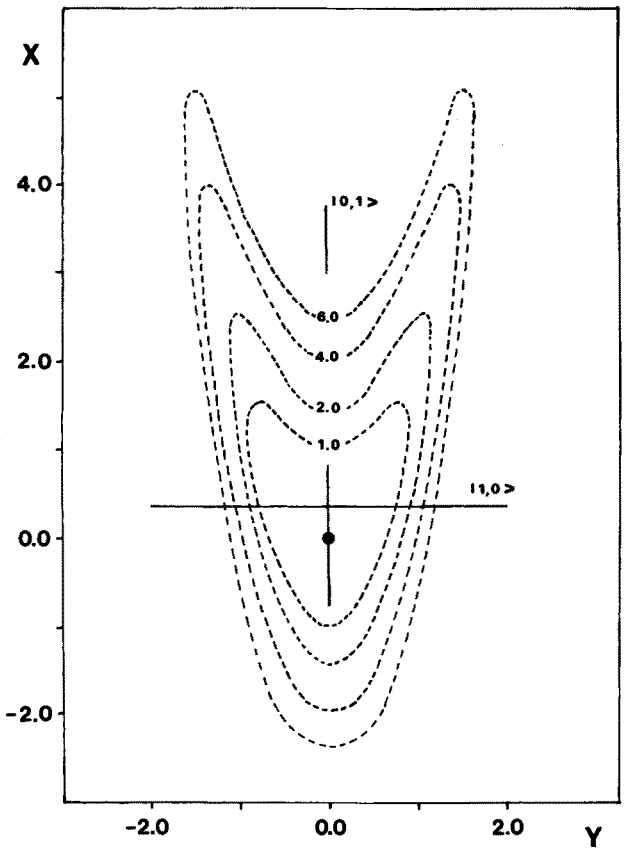

FIG. 3. Potential map of the V_{II} potential as a function of x and y. The nodal lines of the fundamental excited states $|1,0\rangle$ and $|0,1\rangle$ are represented. Distances are mass normalized coordinates, energies in a.u.

Concerning the excited states $|1,0\rangle$ and $|0,1\rangle$, the variational process converges less rapidly than for the $|0,0\rangle$ (see, e.g., Table II). Although convergence is, nevertheless, reached easily with a two-dimensional potential, serious difficulties of memory size may arise for problems of higher dimension. In our case, the convergence has been extended enough (10^{-2} cm^{-1}) to consider our results as exact numerical solutions. Now we can deduce, in the framework of the QMC solutions, the following important properties concerning the nodal lines of fundamental excited states; first we may note that all the energies of the $|1,0\rangle$ and $|0,1\rangle$ states of the studied model potentials are very well reproduced by the QMC calculations. This shows that the choice of the analytical form given in Eq. (27) for the nodal line of a fundamental excited state is appropriate. We may conclude that such states may be reached by partitioning the full space into two subdomains. A more surprising result concerns the shape of the node of the nonsymmetrical $|1,0\rangle$ states: in each case where it is the lowest excited state of the spectrum the parameter α is found to be zero and therefore the node is a straight line, translated from the origin by x_N. We give on Fig. 3 the potential map associated to V_{II} together with the nodal lines of the excited state wave functions $|0,1\rangle$ and $|1,0\rangle$. As explained above, in order to see if this particularity is also true for higher excited (though fundamental) states, we calculated the $|1,0\rangle$ energy of the potential V_{IV} whose lowest excited state is the symmetrical $|0,1\rangle$ level. In that

TABLE II. Energies (cm^{-1}) of the ground and fundamental excited states for the model potential $V_{II}(x,y)$.[a]

State $\|x,y\rangle$	$\|0,0\rangle$	$\|1,0\rangle$	$\|0,1\rangle$
Harmonic	169.0	338.1	338.1
Variational			
n[b] = 2	288.5	532.5	930.4
4	221.1	387.4	531.8
6	213.1	373.2	485.3
8	211.7	367.5	478.0
10	211.0	365.5	475.1
12	210.6	365.0	473.0
14	210.4	364.9	471.9
16	210.3	364.8	471.4
18	210.3	364.7	471.3
20	210.3	364.7	471.2
22	210.3	364.7	471.2
QMC[c]	210.0 ± 1.0	364.7 ± 1.3	472.1 ± 1.1
Parameters[d]		$\alpha = 0.0$	$\alpha = 0.0$
		$x_N = 0.37$	x_N[e] $= 0.0$

[a]QMC calculations have been performed using 40 trajectories with 500 000 elementary time steps. The time step used is 0.01 a.u.
[b]The size of the basis set is $n \times n$.
[c]Our results.
[d]Optimized parameters of the nodal line defined in Eq. (35).
[e]The notation y_N would be better. However, our convention here is to denote x_N the translation parameter associated with the excited vibration (y in this case).

case, there may be a very weak distortion of the nodal line. We give in Table III the QMC energy values for this state corresponding to $\alpha = 0.0$ and -0.02, respectively. In that case, even if the nodal line is slightly distorted, we show that the straight line approximation is good. From Table III, we can see that the increase of the coupling between V_I and V_{II} leads, as expected, to an increased value of x_N. Concerning the symmetrical $|0,1\rangle$ states, the predicted values of the pa-

TABLE III. Vibrational energies of the ground and fundamental excited states of some model and realistic potentials.[a]

Potential	State	Var.	QMC	α	x_N[b]
I	$\|0,0\rangle$	192.8	192.8 ± 0.3	...	...
	$\|1,0\rangle$	359.8	359.8 ± 0.2	0.0	0.125
	$\|0,1\rangle$	436.6	437.1 ± 0.5	0.0	0.0
II	$\|0,0\rangle$	210.3	210.0 ± 1.0	..	...
	$\|1,0\rangle$	364.7	364.6 ± 1.5	0.0	0.368
	$\|0,1\rangle$	471.2	472.1 ± 2.2	0.0	0.0
III	$\|1,0\rangle$	447.4	448.3 ± 1.1	0.0	0.164
IV	$\|1,0\rangle$	618.1	619.0 ± 0.9	-0.02	0.093
			619.3 ± 0.9	0.0	0.088
h,r	$\|0,0\rangle$	356.7	356.7 ± 0.1	...	...
	$\|1,0\rangle$	877.8	877.3 ± 0.1	0.0	0.053
	$\|0,1\rangle$	548.7	548.7 ± 0.2	0.0	0.044
h,z	$\|0,0\rangle$	247.5	247.9 ± 0.5	...	...
	$\|1,0\rangle$[c]	648.4	645.0 ± 0.6	0.0	0.067
	$\|0,1\rangle$	312.7	313.6 ± 1.1	0.0	-0.072

[a]All energy values are in cm^{-1}.
[b]In atomic units with mass normalized coordinates.
[c]See Fig. 7.

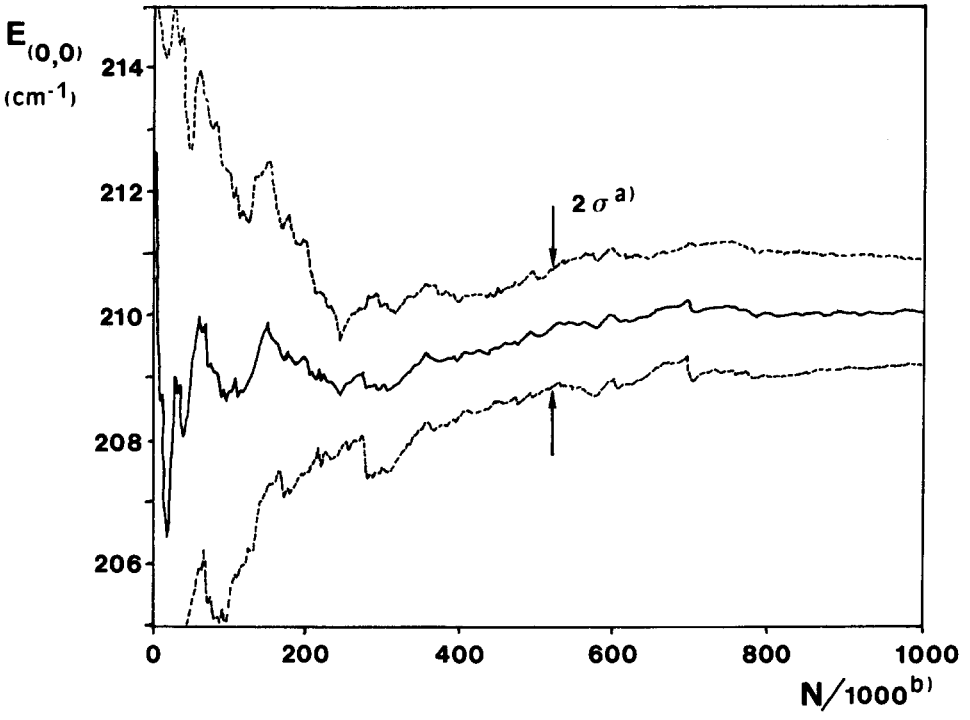

FIG. 4. Estimator of the ground state energy as a function of the simulation time for the V_{II} model potential. σ is the standard deviation. A set of 40 trajectories is divided into 10 subsets of 4 trajectories and σ is evaluated from the dispersion of the ten corresponding energies calculated for each subset. N is the number of time steps for each trajectory. The CPU simulation time is directly proportional to N.

rameters α and x_N (zero) are reproduced. Finally, to illustrate our algorithm, we present in Fig. 5 the dependency of $E_{FN} = \min(\epsilon_1,\epsilon_2)$ with respect to x_N for symmetrical ($|0,1\rangle$ state of V_I) and unsymmetrical ($|1,0\rangle$ state of V_{II}) states. Clearly, E_{FN} is very dependent on the partitioning of the space and then the desired equality $\epsilon(\alpha) = \epsilon_1 = \epsilon_2$ is obtained very easily. Note that the asymptote of the curve $E_{FN}(x_N)$ gives the ZPE since $\lim_{x_N \to \infty} \varphi_0^{(0)}$ is a nodeless function. Finally, the extremum principle is represented in Fig. 6 for the unsymmetrical $|1,0\rangle$ state of V_{II}. It shows clearly that the minimum is obtained for $\alpha = 0.0$. Furthermore, the correlation between the two parameters is clear: as α increases (from -0.5 to $+0.5$ on Fig. 6) and tends to unbalance the two subdomains, x_N decreases to compense this effect.

B. $Pd_{14}CO$

Calculated energies of vibrational states for the two types of coupling are presented in Tables III and IV. Different approaches are compared with QMC, namely, the crude harmonic approximation (one-dimensional approximation) the PNC representation and the variational procedure. The effect of the basis set size on the $|1,0\rangle$ excited state energy is also illustrated by Fig. 7 for the h,z coupling. The ground state energies in these simple two-dimensional cases are very well reached by variational calculations whereas harmonic approximations (crude and PNC) may give significant errors (see Table IV). For $|0,0\rangle$ states the QMC runs converge very rapidly as a function of the simulation time T. An accuracy better than 1 cm^{-1} is very easy to obtain.

Concerning the first excited state $|0,1\rangle$ of the cluster vibration, the variational convergence is also satisfactory for both couplings, less than 1.0 cm^{-1} from the value given by QMC. In the case of the h,r coupling the optimization of α and x_N shows that the nodal line is slightly translated. This reflects the slight difference between PNC and exact QMC results (about 1 cm^{-1}) which results from both anharmonic and coupling terms of the potential. In the case of the $|0,1\rangle$ state of the h,z coupling, the nodal line is a little more translated. Hence, the difference between PNC and exact QMC results (about 20 cm^{-1}) is larger.

The variational treatment of the $|1,0\rangle$ excited state of the h,z coupling (the adsorbate-surface vibration) is more difficult. A few comments on the rather erratic behavior of the variational results for $|1,0\rangle$ may be in order. The first concerns the lack of monotonic convergence seen for the h,z calculations (Fig. 7) upon increasing the size of the basis set. In fact the Hylleraas–Undheim–MacDonald theorem[20–22] ensures that in a linear variational calculation the mth lowest root is never lower than the mth exact eigenvalue of the Hamiltonian. This theorem is of course satisfied for our calculations. The fact that the energy of the $|1,0\rangle$ state (identified by its eigenvector) sometimes increases when basis functions are added reflects the existence of lower lying states (overtones $|0,v\rangle$ of the z vibration). If the added basis functions can better describe these overtones than the $|1,0\rangle$ state then a change in the order of the approximate excited-state energies can occur and the accuracy of the $|1,0\rangle$ level can deteriorate. This is the case for the h,z coupling when the basis set size goes from 10×10 to 12×12 (see Fig. 7). In that case the overtone $|0,4\rangle$ reaches an energy lower than the $|1,0\rangle$ fundamental excited state whose energy increases. If the convergence of the $|1,0\rangle$ state associated with the h,r potential is obtained easily (both QMC and variational treatments lead to very close results), that is not the case for h,z. The explanation involves the fact that the potential has been fitted by a polynomial and hence does not have the correct asymptotic form. The eigenvalues of this fit to the

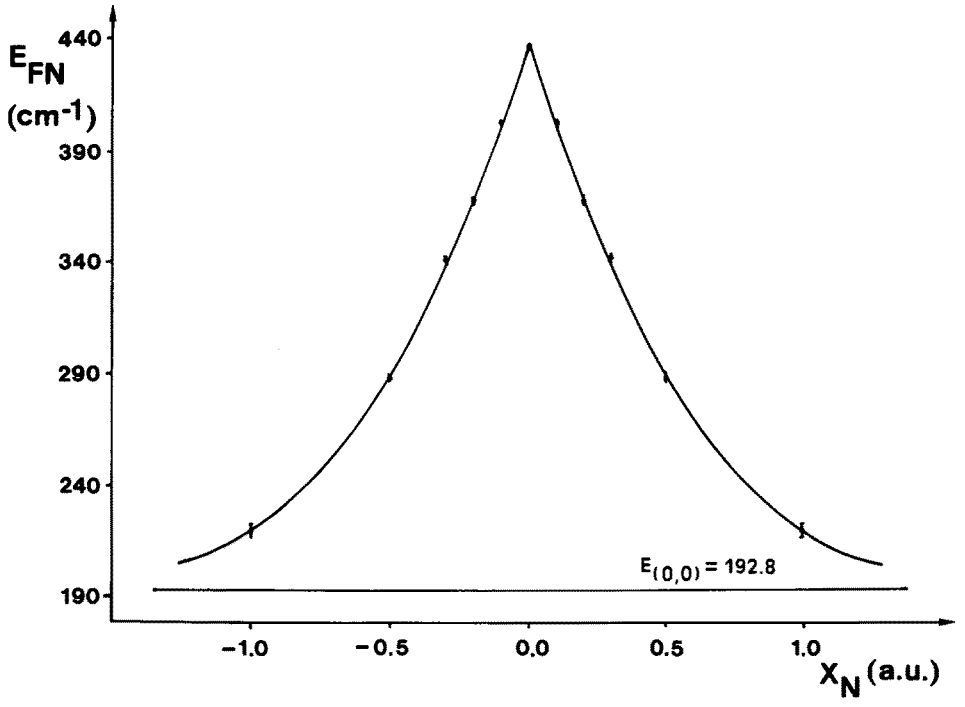

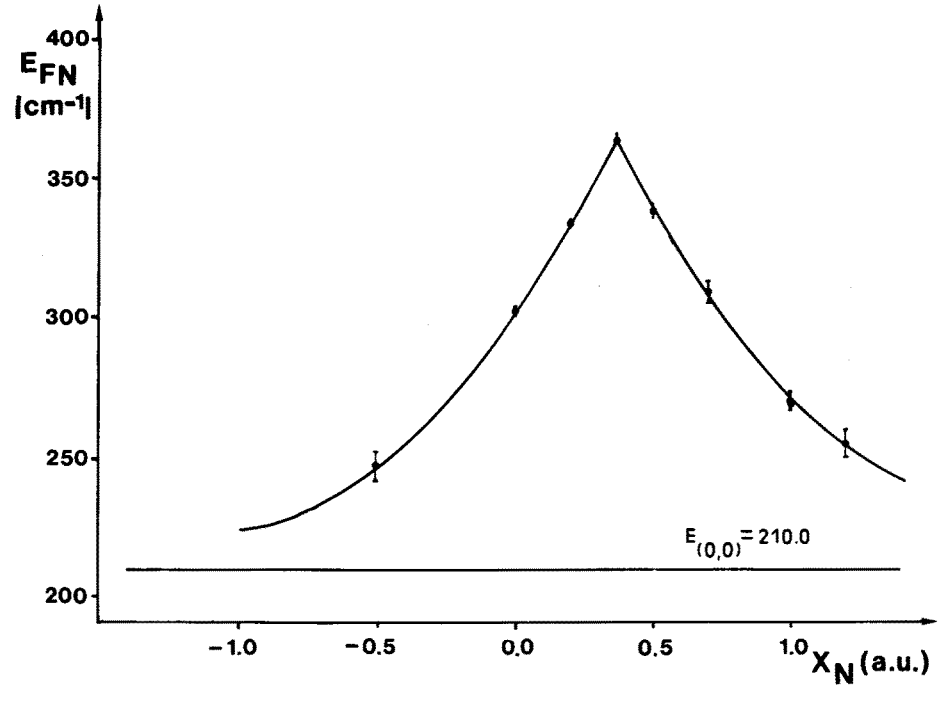

FIG. 5. Fixed-node energy of (a) the $|0,1\rangle$ state of the $V_{\rm I}$ potential (symmetrical case, optimized value of x_N is 0.0) and (b) the $|1,0\rangle$ state of the $V_{\rm II}$ potential (unsymmetrical case, optimized value of x_N is 0.368), vs the translational parameter x_N.

potential are determined by the arbitrary tail as well as by the physically interesting region near the minimum. If only low-order functions are included in the variational calculation (say $n = 5, 7$), functions which have negligible weight in the pathological region of the potential fit, then an upper bound to the physical eigenvalue will be attained. Adding higher-order, more long-range basis functions eventually allows convergence to the exact (but unphysical) eigenvalue of the fitted potential. In order to improve the physical eigenvalue, we chose to contract sufficiently the basis set functions in the physical region of the potential in order to extend the convergence process as far as possible. In that case, the long-range effects are avoided, but on the other hand, the convergence is slow as shown in Fig. 7. By contrast, the QMC procedure using only local behavior of the potential around the equilibrium position works well in this case and then illustrates its efficiency. To summarize, we can say that in the variational process, a large extension of the basis set is needed to describe as well as possible the wave function in the neighborhood of the physical potential, but at the same time it would increase the contribution of the "nonphysical" region of V; on the other hand, it is always possible with the QMC to choose the reference function to prevent the trajectories (through the drift vector) from visiting the wrong region of

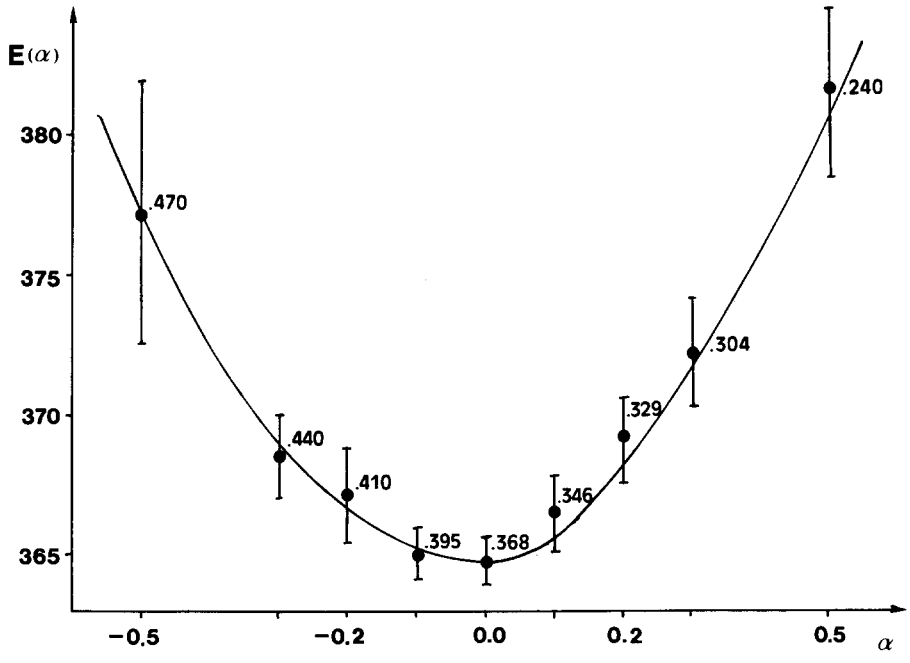

FIG. 6. Illustration of the extremum principle for the $|1,0\rangle$ state of the V_{II} potential. At each point of the curve, we give the value of the translational parameter x_N which assures the equality $\epsilon_1 = \epsilon_2 = \epsilon(\alpha)$ (see Figs. 5).

V during the simulation time. It is then possible to satisfactorily describe the metastable states of the whole potential. However, as already emphasized, a much more satisfactory approach would consist in using a physical representation for V having the correct asymptotic behavior, instead of a polynomial fit. This nonphysical fit is used only because the purpose of this paper is to compare both variational and Monte Carlo treatments. In our example (see Table III), we deduce that the QMC improves the $|1,0\rangle$ energy by 3.4 cm^{-1} on the best variational result. The QMC value is presented in Fig. 7 as the asymptote of the variational process. For both couplings the nodal line is a straight line ($\alpha = 0$). Finally, each of the nodal lines of the excited states of the two realistic potentials studied here are "undistorted" as was also found for the model potentials. In Table IV, the corresponding vibrational frequencies are quoted.

C. Pd_2CO

As a second example where the accuracy and stability of the QMC approach have proven crucial, we briefly present a few results from a preliminary study of the effect of an external electric field on the CO stretch vibration of the Pd_2CO cluster. We have studied the coupling of this d mode with the

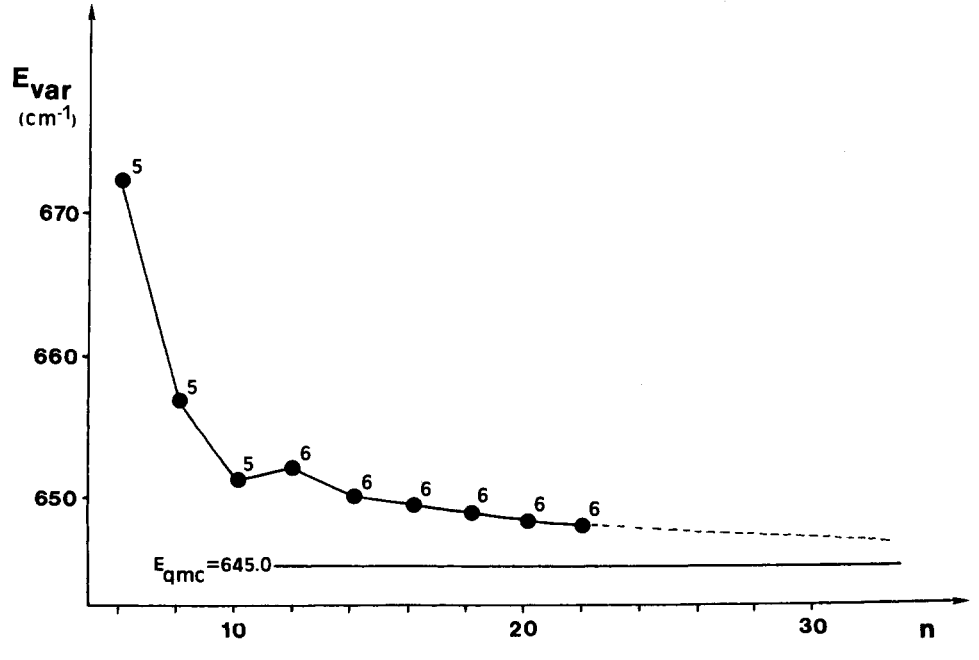

FIG. 7. Convergence of the variational process with respect to the basis set size, $n \times n$, for the $|1,0\rangle$ state of the h,z coupling. At each point, we give the sequence number of the $|1,0\rangle$ root.

TABLE IV. Vibrational frequencies[a] (cm^{-1}) of the two coupled modes h,r and h,z.

Method	Harmonic	PNC	Variational[b]	QMC[c]
Coupling				
ω_r[d]	240.0	192.8	192.0	192.0 ± 0.3
ω_h[d]	498.0	504.9	521.1	520.6 ± 0.2
ω_z[d]	195.7	86.7	65.2	65.7 ± 1.6
ω_h[d]	498.0	544.4	400.9	397.1 ± 1.1

[a]Evaluated from Tables III.
[b]The size of the basis set is 22×22.
[c]Our results.
[d]$\omega_h = E_{(1,0)} - E_{(0,0)} \cdot \omega_{r/z} = E_{(0,1)} - E_{(0,0)}$.

adsorbate-surface h mode. Table V shows the results of a convergence study for variational calculations in the field-free case. The overall variations of the frequencies as a function of $2 \leqslant l \leqslant 6$ (l is the polynomial order) and of $6 \leqslant n \leqslant 20$ (the size of the basis set) are about 50 cm^{-1} for the d vibration and about 10 cm^{-1} for h. Although this could be a useful level of accuracy in many contexts, the frequency shifts as a function of field in which we are interested are of the same order of magnitude.[23] We are in a case where the convergence of the variational treatment seems satisfactory. However, the results show the sensitivity of the excitation energies to the polynomial order. It is another example of the necessity to fit the potential by a more physical analytical form. As already noticed, this may be done straightforwardly with the QMC procedure. In order to compare the two methods we decided to use a polynomial fitting at the fourth order ($l = 4$) and the variational results obtained with $n = 20$. Variational and QMC results are shown in Table VI for values of an external electric field appropriate for an electrochemical study. Although the differences in frequencies between the variational and QMC approaches are at most about 10 cm^{-1} ($\cong 0.5\%$) and the qualitative trend as a function of electric field is the same in both cases, there are significant quantitative differences. In particular the variational calculations yield quite different results for fields of the same

TABLE V. Excitation energies (cm^{-1}) ($v = 0 \rightarrow v = 1$) for the C–O (d) (top numbers) and Pd_2–CO (h) (bottom numbers) vibrations of Pd_2CO in absence of electric field.

Polynomial order[a] / n[b] l	6	10	16	20
2	1923	1923	1907	1908
	505	504	505	505
3	1899	1888	1874	1875
	501	500	499	499
4	1898	1890	1873	1873
	495	495	495	495
5	1894	1881	1866	1866
	500	500	500	500
6	1920	1915	1911	1913
	498	497	497	497

[a]Potential fit with $V(x_1, x_2) = \Sigma_{i+j \leqslant l} a_{ij} x_1^i x_2^j$.
[b]The size of the basis set is $n \times n$.

TABLE VI. C–O stretching frequency (cm^{-1}) vs electric field ($V/cm \times 10^7$) for Pd_2CO calculated by variational and by quantum Monte Carlo (QMC) methods.

	ω_{CO}			$\Delta\omega_{CO}/\Delta E$[a]		
Method	PNC	Var.	QMC[b]	PNC	Var	QMC[b]
Electric field ($V/cm \times 10^7$)						
−5.0	1871	1833	1833			
−2.5	1899	1859	1855	28	26	22
0.0	1914	1873	1878	15	14	23
2.5	1949	1908	1900	35	35	22
5.0	1969	1927	1920	20	19	20
10.0	2000	1961	1949	15.5	17	14.5

[a]ΔE is taken as $2.5\ V/cm \times 10^7$.
[b]For each QMC value, the variance is lower than 0.5 cm^{-1}.

magnitude but opposite sign whereas the QMC frequency shifts are nearly symmetrical. In fact, the experimental electrochemical curves, frequency vs voltage, have a symmetrical sigmoïd shape. Given the uncertainties of the cluster model and of the electrochemical double layer, etc., this does not in itself prove the superiority of QMC; however, taken together with the convergence difficulties of the variational approach we believe that QMC affords clear advantages for this type of problem.

VI. CONCLUSIONS

The results presented here show the efficiency of the FGFK-QMC method applied to two-mode vibrational problems when considering zero-point energy and fundamental excitations. The extension to many-mode problems is straightforward. Furthermore the results emphasize the difficulty of obtaining convergence for variational calculations when the coupling and anharmonicity parts of the interaction are nonnegligible. In that case a large number of basis states is required; however it is clear that if the number of coupled vibrations increases, variational solutions become unfeasible due to the size of the basis set needed. No such limitation arises with the QMC approach; the essential condition in this case is to find a fair reference function in order to reduce the computer time. This last point appears to be made easier by the remarkable properties of the approximate nodal surfaces associated with the fundamental excited states: (i) The partition of space into two and only two subdomains (independently of the sequence number of the state) seems to lead to satisfactory results. (ii) Their distortion seems to reduce to nearly a translation. If such strong assumptions always lead to very good results, then a potentially important criticism of the method, namely the more or less complicated parametrization of the nodal surface, disappears. Nevertheless, this point needs to be verified for larger systems. Another aspect of the difficulties encountered with the variational treatment is related to the analytical representation of the potential. In practice, the only analytical forms used are polynomial expansions which permit straightforward evaluation of Hamiltonian matrix elements. Unfortunately, such expansions can efficiently represent

only potentials where anharmonicity and coupling are weak. Furthermore, the wrong asymptotic behavior of these fitted analytical potentials does not allow the use of large delocalized basis sets. QMC entirely avoids these problems, since no specific constraints resulting from the potential are introduced. Furthermore, it is even possible to introduce a locally interpolated numerical form of the potential into the numerical process. Consequently, this method appears well-adapted for studying strongly coupled interactions as well as multiple-well potentials.

ACKNOWLEDGMENTS

This work was partially supported by grants from NSERC (Canada, operating and supercomputer access), FCAR (Québec), and the Institut Français du Pétrole for which we are grateful. D.R.S. wishes to acknowledge a stimulating conversation with Mark Wrighton. M.C., P.C., and C.M. thank the "Conseil Scientifique du Centre de Calcul Vectoriel pour la Recherche" for providing them with computer facilities and are indebted to the "Centre de calcul d'Orsay" for allowing them to make use of facilities on the NAS 9080 and the IBM 3090/200.

[1]R. J. Whitehead and N. C. Handy, J. Mol. Spectrosc. **55**, 356 (1975).
[2]F. Soto-Eguibar and P. Claverie, in *Stochastic Processes Applied to Physics and Other Related Fields*, edited by B. Gomez, S. M. Moore, A. M. Rodriguez-Vargas, and A. Rueda (World Scientific, Singapore, 1983), p. 637–649.
[3]M. Caffarel and P. Claverie, J. Stat. Phys. **43**, 797 (1986).
[4]M. Caffarel and P. Claverie, J. Chem. Phys. **88**, 1088 (1988).
[5]M. Caffarel and P. Claverie, J. Chem. Phys. **88**, 1101 (1988).
[6]E. B. Wilson, J. C. Decius, and P. C. Cross, *Molecular Vibrations* (Dover, New York, 1955).
[7]P. J. Reynolds, D. M. Ceperley, B. J. Alder, and W. A. Lester Jr., J. Chem. Phys. **77**, 5593 (1982).
[8]D. M. Ceperley and B. J. Adler, J. Chem. Phys. **81**, 5833 (1984).
[9]H. Risken, *The Fokker–Planck Equation* (Springer, Berlin, 1984).
[10]M. H. Kalos, *Monte Carlo Methods in Quantum Problems*, NATO ASI Series C (Reidel, Dordrecht, 1982), pp. 19–31.
[11]D. M. Ceperley, in *Recent Progress in Many–Body Theories*, edited by J. G. Zabolitzky, M. deLlano, M. Fortes, and J. W. Clark (Springer, Berlin, 1981), p. 262.
[12]L. D. Landau and E. Lifshitz, *Quantum Mechanics* (Pergamon, Oxford, 1965), Chap. 3, Sec. 20.
[13]M. Caffarel, Thése de Doctorat de l'Université Paris VI, 1987.
[14]J. Andzelm and D. R. Salahub, Int. J. Quantum. Chem. **29**, 1091 (1986).
[15]J. Andzelm and D. R. Salahub, in *Physics and Chemistry of Small Clusters*, edited by P. Jena, B. K. Rao, and S. N. Khamma, NATO ASI Series B158 (Plenum, New York, 1987), p. 867.
[16]J. Andzelm, D. R. Salahub, M. Caffarel, P. Claverie, and C. Mijoule (unpublished).
[17]J. Andzelm, E. Radzio, and D. R. Salahub, J. Chem. Phys. **83**, 4573 (1985).
[18]C. Mijoule, M. Allavena, J M. Leclercq, and Y. Bouteiller, Chem. Phys. **109**, 207 (1986).
[19]For one-dimensional systems it is known (see Ref. 12, Chap. 3, Sec. 21) that the k th excited state has just k nodes which divide the configuration space (the real line) into just $(k+1)$ subdomains. This property admits a weaker generalization for an N-dimensional configuration space proved by Zhislin [G. M. Zhislin, Usp. Mat. Nauk **16**, 149 (1961)]. This theorem states that the nodal hypersurfaces of the k th excited state divide the N-dimensional configuration space into *at most* $(k+1)$ subdomains.
[20]E. A. Hylleraas and B. Undheim, Z. Phys. **65**, 759 (1930).
[21]J. K. L. MacDonald, Phys. Rev. **43**, 830 (1933).
[22]J. P. Lowe, *Quantum Chemistry* (Academic, New York, 1978), Appendix 4.
[23]K. Kunimatsu, J. Phys. Chem. **88**, 2195 (1984).